Convection Cells and Segregation in a Vibrated Granular Bed

Shu-San Hsiau, Pai-Chei Wang, and Chi-Hwang Tai
Dept. of Mechanical Engineering, National Central University, Chung-Li, Taiwan 32054, R.O.C.

Granular materials may be circulated in a container with two symmetric convection cells under external vertical vibration conditions. Effects of the container geometry on the convection strength and segregation process are studied experimentally. First, the wall tilted outward angles are changed to observe the direction of the convection roll and convection strength. The strength of the normal convection rolls decreases by increasing the wall angles of the container from 0° (vertical walls). The convection rolls become reversed when the wall tilted outward angles are greater than a transition angle. The wall roughness and vibration velocity amplitude are also changed to investigate their influences on the convection cell strength. The segregation of a larger disk induced by the convection cells of smaller disks shows that the normal convection rolls induce the upward motion of the larger disk, and the reverse convection rolls result in the downward motion of the larger disk. The separation velocity increases linearly with the convection flow rate.

Introduction

Granular material is an assembly of discrete solid particles dispersed in an interstitial fluid. Granular material flows have wide applications in industries, such as the transport of coal, ore, plastics, grains, mineral concentrates, sand, powders, food products, or pharmaceuticals. Shakers are important devices to mix and dry granular materials in industries (Suzuki et al., 1980; Pakowski et al., 1984; Yu et al., 1992). Shakers are also used to sort granular materials according to particle size in pharmaceutical, powder metallurgy, and food industries. Jaeger and Nagel (1992) presented a good review of the related studies which investigated the phenomena of granular systems under vibration. Many studies show that a granular bed can be fluidized and several different kinds of complicated phenomena under external vibrations can be generated (Hsiau and Pan, 1998; Wassgren et al., 1996). These phenomena include heaping (Clément et al., 1992; Evesque and Rajchenbach, 1989; Fauve et al., 1989; Lee, 1994; Wassgren et al., 1996), convection (Laroche et al., 1990; Taguchi, 1992), fluidization (Clément and Rajchenbach, 1991; Ichiki and Hayakawa, 1995; Luding et al., 1994; Warr et al., 1995), size segregation (Hsiau and Yu, 1997; Jullien et al., 1992; Knight et al., 1993; Rosato et al., 1987), surface wave (Melo et al., 1994; Pak and Behringer, 1993; Wassgren et al., 1996) and arching (Douady et al., 1989; Hsiau et al., 1998; Wassgren et al., 1996). The convection of granular materials is an important driving mechanism for these interesting phenomena (Taguchi, 1992; Knight et al., 1993; Gallas et al., 1992). No flow occurs when the vertical vibration acceleration amplitude falls below a threshold (1.2 g, where g is the gravitation acceleration), and the granular bed system behaves as a solid body. When the vibration acceleration is above the threshold, convective flow occurs and the granular system is fluidized. It indicates the translation of the granular bed from a consolidation state to a fluid-like state. Under some conditions, the flow of granular materials between the top and bottom occurs in the form of convection cells (convection rolls) (Gallas et al., 1992; Knight et al., 1996). The convection phenomena attracted many researchers in this decade. Gallas et al. (1992) used a molecular dynamics method to study the convection cells in a two-dimensional (2-D) system. They found different types of convection cells because of the existence of walls or the vibration amplitude. Taguchi (1992) studied the convection cells numerically and proposed that the convection cells were induced by elastic interaction between particles. Molecular dynamics was employed by Luding et al. (1994) to investigate the convection cells of vibrated grains. They claimed

Correspondence concerning this article should be addressed to S.-S. Hsiau.

that the molecular simulations might use parameters leading to unphysically large contact time between particles that resulted in the enhancement of the appearance of convection cells. Wassgren et al. (1996) used 2-D discrete element simulations to examine the convection cell phenomena in a shaker with vertical side walls. The influences of aspect ratio on the convection cell type, the locations of convection center, and the particle flow rate were studied. Hayakawa et al. (1995) studied the convection rolls by using a hydrodynamic model. They concluded that the instability mechanism led to the convection cells.

There have been relatively few experimental studies about the convection cells generated in a shaker. Knight et al. (1996) investigated poppy seeds in cylindrical containers subject to discrete vertical tapes. Magnetic resonance imaging (MRI) was employed to study the behavior of the convection cells in the bed. The vertical flow velocity profiles at different heights were measured. The radial dependence of the velocity profiles could be approximated by a hyperbolic cosine or a modified Bessel function of order zero. Knight (1997) employed similar experimental technology to analyze the convection rolls in different external boundaries. The directions of the convection rolls could be reversed when the side walls were titled outwards over a critical angle, and a similar conclusion was verified by a tool of a computer simulation method (Grossman, 1997). Hsiau and Chen (2000) used a particle tracking method to investigate the flow fields of the convection cells and found a power law existing between the convection strength and the vibration velocity amplitude.

There are two mechanisms causing segregation in a shaker: reorganization and convection (Barker and Metha, 1993). The granular materials undergo a transition from a dense (solid-like) state to a dilute (liquid-like) state (Hsiau and Yu, 1997; Knight et al., 1997). During the bed expansion process, the larger voids among particles are formed causing the reorganization of particles, and the smaller particles are more easily falling down through the voids to the bottom (Barker and Metha, 1993; Hsiau and Yu, 1997; Rosato et al., 1987). The reorganization mechanism disappears at a very low vibration acceleration since there are not enough relative movements among particles to cause larger voids. When the vibration acceleration is too high, the voids are so large that the larger particles can also fall down through the voids; therefore, there is also no segregation phenomena in the granular bed (Hsiau and Yu, 1997).

Knight et al. first proposed that the convection is the main mechanism causing size separation in a vibrated granular bed (Knight et al., 1993, 1997). The particles flow upwards in the center of the container and fall down along the side walls in a thin stream. The larger particles are brought by the convection cell to the bed top and remain there. Barker and Metha (1993) analyzed the importance of the particle rearrangement mechanism and the convective mechanisms. They pointed out that the amplitude, frequency, and acceleration of vibration are important factors to determine the dominant mechanism in the segregation process.

This article intends to change the container geometry and the friction coefficient of the side walls to investigate the convection cells of granular disks under external vibration. The effect of the convection cells on the segregation of granules is also discussed in this article.

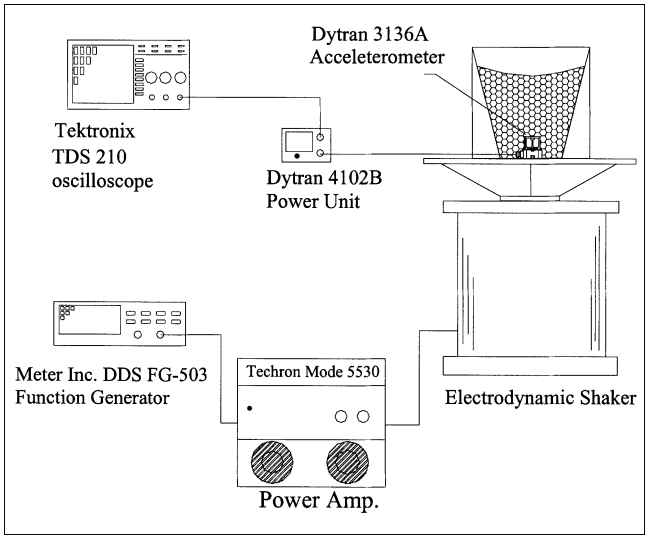

Figure 1. Current experimental apparatus.

Experimental Setup

Figure 1 shows the experimental apparatus. A Techron VTS-100 electromagnetic vibration system was served as the vertical shaker. The shaker was vertically driven by sinusoidal signals produced by a function generator (Meter DDS FG-503) through a power amplifier (Techron 5530). The vibration frequency f and acceleration a were measured by a Dytran 3136A accelerometer that was fixed at the shaker and was connected to an oscilloscope (Tektronix TDS 210). The vibration radian frequency ω and amplitude r could be calculated from $\omega = 2\pi f$ and $r = a/\omega^2$. The dimensionless acceleration amplitude Γ and the dimensionless velocity amplitude V_b were defined as $\Gamma = a/g$ and $V_b = r\omega/(gd)^{1/2}$, where d is the average disk diameter. The dimensionless acceleration amplitude Γ is fixed at 4 in this article.

The current experiments used bronze disks (thickness of 3 mm, density ρ_p of 8,780 kg/m^3) as granular materials. There were 450 bronze disks (225 disks with a diameter of 4 mm and 225 disks with a diameter of 5 mm; $d = 4.5$ mm) prepared for each experimental test. 18% of the disks were served as tracer particles which were dyed with white color. A tank, with glass plates as the front and back walls and with plexiglass as the side and bottom walls, was driven by the shaker. There were seven containers with different tilted angles of side walls, θ_{wall} (0°, 6°, 8°, 10°, 12°, 14°, and 20°), prepared for the experiments. The height, bottom width, and depth of the inside space of the tanks were 20 cm, 8 cm and 0.35 cm. Therefore, there existed only one layer of bronze disks in the tank and the flow generated in the granular bed was 2-D (x: horizontal coordinate with 0 in the center; y: vertical coordinate with 0 at the bed floor). The surface friction of the side walls is important in generating the complex flow phenomena (Wassgren, 1997). Three different materials were glued to the side walls to make different wall roughness:

Wall 1: No. 100 sandpapers.

Wall 2: The wall glued by a layer of bronze disks with a diameter of 4 mm.

Wall 3: The wall glued by a layer of bronze disks with diameters of 4 mm and 5 mm, in sequence.

The sliding angle θ_s between the granular disks and the side walls was used to characterize the wall roughness. The sliding angle was decided by a simple experiment. A certain amount of the tested disks were placed above a wall with the same tested wall property. The disks slid down when the wall was inclined to a critical angle and the critical angle was defined as the sliding angle of the wall θ_s. The sliding angles for Walls 1, 2, and 3 were 9°, 29°, and 34.3° from the above simple experimental procedure.

As the wall friction influences the flow behavior very much, thus, the front and back glass plates were carefully cleaned and polished before every experimental test to reduce the frictional effect.

A Kodak motion corder analyzer (model SR-Ultra, with a maximum recording speed of 10,000 frames per second) was used to record the flow. The digital images were transported to a personal computer for future analyzing. Every image of the motion was digitized to gray levels (ranging from 0 to 255 due to the different colors of the tracers and the background disks), and stored in a computer file. The autocorrelation technique was employed to process the stored images and to decide the shift of each tracer in every two consecutive images. The details of the autocorrelation process can be found in Natarajan et al. (1995) and Hsiau and Shieh (1999).

The granular bed was divided into many subregions with a height of 0.45 cm (the width is varied because of the shape of the container). The ensemble average velocity vector in each bin was averaged from about 120 to 200 tracer particles taken from 1,000 vibration cycles. Note the average velocity calculated here was called the long-term average velocity (Wassgren, 1997), which was determined from the particle displacements per vibration cycle. Errors in the long-term velocities are less than 4%. The errors primarily result from the uncertainty in determining the centroid of the tracer particles. A correlation experiment was also done by attaching particles on the front wall of the vibrated container. The long-term velocities in vertical and horizontal directions should be 0. The ratios of these velocities to the vibration velocity amplitude ($r\omega$) by employing the above procedures are less than 1%.

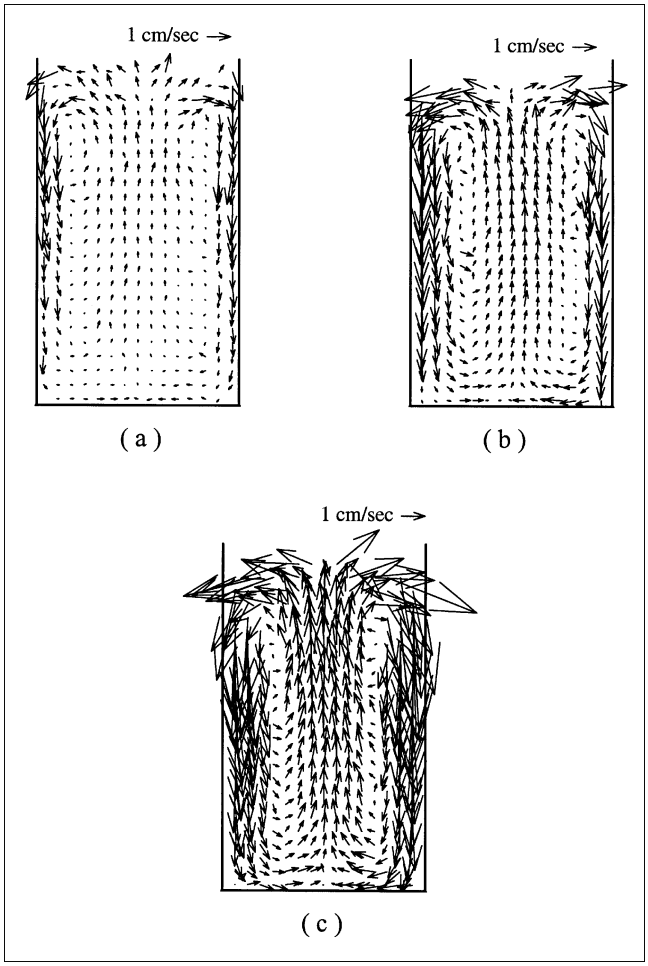

Figure 2. Velocity fields of granular beds of rectangular container ($\theta_{wall} = 0°$).

(a) Wall 1; (b) Wall 2; (c) Wall 3, as the side walls of the granular beds, $\Gamma = 4$; $V_b = 2$.

Results and Discussions

Influences of the container geometry and the wall friction

There are seven containers with different tilted angles of side walls, θ_{wall} (0°, 6°, 8°, 10°, 12°, 14°, and 20°), prepared for the experiments. Three walls with sliding angles θ_s of 9°, 29°, and 34.3° are used as the side walls. The dimensionless vibration acceleration and velocity are fixed at $\Gamma = 4$ and $V_b = 2$.

Figures 2a to 2c show the velocity fields of the granular beds of a rectangular container ($\theta_{wall} = 0°$) with Walls 1, 2, and 3 as the side walls. Two convection symmetric cells are found in the vibrated bed. The granular materials move upward in the central part and move downward along the side walls of the container. Grossman (1997) reffered to this side wall convection phenomenon as "normal convection." The influence of the frictional effect on the convection cells can be clearly seen from Figures 2a to 2c. With the rougher wall surface (greater sliding angle of the side walls), the convection of the disks is more significant. The rise in the circulation velocity is noteworthy for the case using Wall 3.

Lee (1994) and Grossman (1997) have discussed the mechanism causing the heap formation and convection rolls under the vertical vibration. Along the side walls, the shear force is larger for the upward phase during a vibration cycle; at that time, the granular bed is in a more densely packed state. Since the shear force plays the role of a drag force on the particles, the particles can therefore move faster for the downward phase. The above mechanism induces the net downward movement of particles along the side walls. Those particles moving to the bottom along the side walls return to the top from the central bed. Therefore, the normal convection cells are formed in the bed.

Using Wall 1 as the side walls ($\theta_s = 9°$), Figures 3a to 3f show the velocity fields of the granular materials with the side walls rotating outwards ($\theta_{wall} = 6°$, 8°, 10°, 12°, 14°, and 20°). For the case of $\theta_{wall} = 6°$, the convection cells are similar to the rectangular container ($\theta_{wall} = 0°$, Figure 2a), but the velocity scales are smaller indicating that the convection strength decreases with the increase of θ_{wall}. From Figure 3b where $\theta_{wall} = 8°$, the directions of two convection cells reverse. The granular materials move downwards in the center

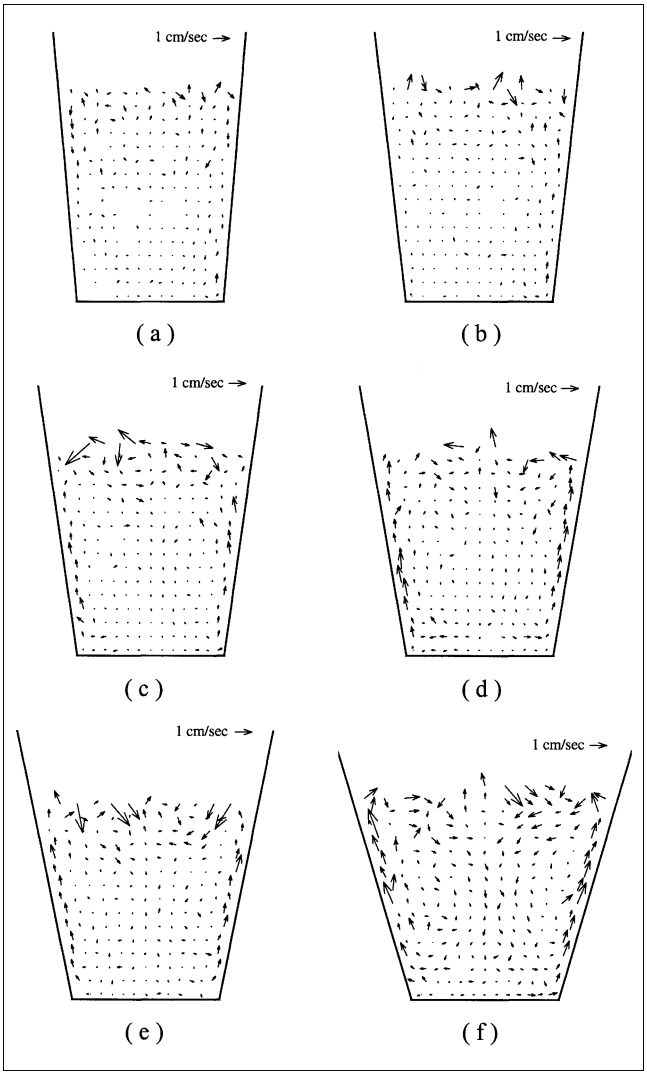

Figure 3. Velocity fields of the granular bed with Wall 1 as side walls rotating outward.

$\Gamma = 4$; $V_b = 2$, θ_{wall} = (a) 6°, (b) 8°, (c) 10°, (d) 12°, (e) 14°, (f) 20°.

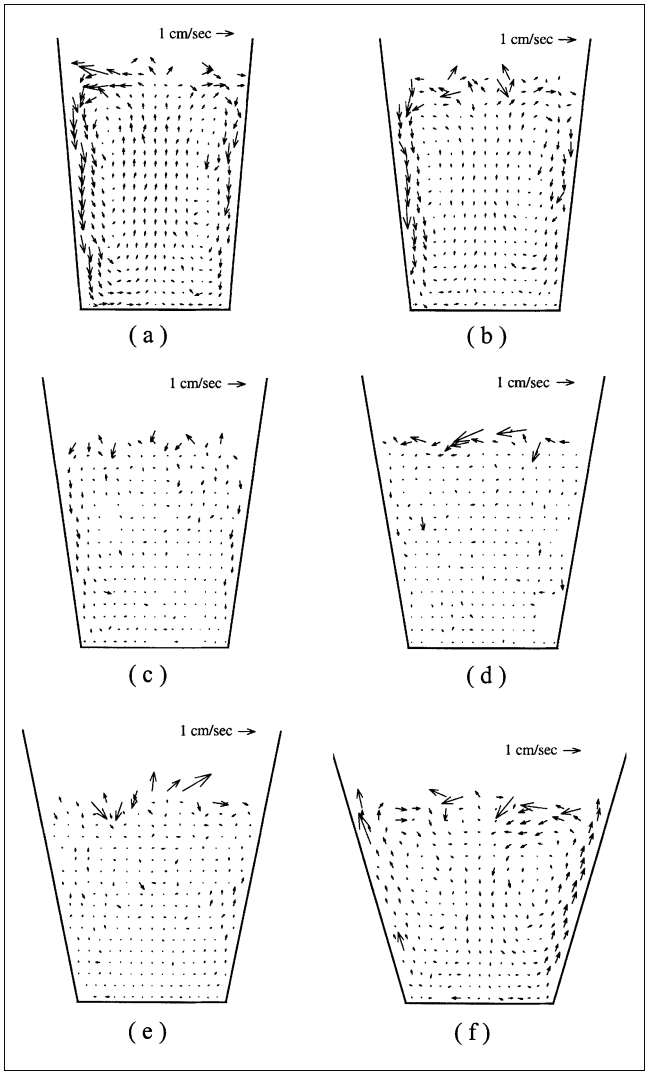

Figure 4. Velocity fields of the granular bed with Wall 2 as side walls rotating outward.

$\Gamma = 4$; $V_b = 2$, θ_{wall} = (a) 6°, (b) 8°, (c) 10°, (d) 12°, (e) 14°, (f) 20°.

and move upward along the side walls. With the increase of θ_{wall}, the velocity magnitudes of the reversed convection cells increase.

Figures 4a to 4f show the velocity fields of the vibrated bed using Wall 2 as the side walls ($\theta_s = 29°$) for different wall angles ($\theta_{wall} = 6°$, 8°, 10°, 12°, 14°, and 20°). The downward movements of disks along the side walls can be clearly observed from Figures 4a to 4c. Two normal convection cells exist in the bed. The strength of the normal convection decreases with the increase of θ_{wall}. With the wall angle of 12°, the velocity scales along the side walls are relatively small, as shown in Figure 4d. Although there are few vectors downward, many regions along the side walls have no velocity vectors. It indicates that the convection cells start to reverse in this geometry of container. For θ_{wall} of 14° and 20°, the reversed convection cells are clearly seen in Figures 4e and 4f. The convection strength is larger for the case of $\theta_{wall} = 20°$.

The velocity fields of the bed using Wall 3 as the side walls ($\theta_s = 34.3°$) are shown in Figures 5a to 5f. The normal convection cells exist in the bed with $\theta_{wall} = 6°$, 8°, 10°, 12°, and 14°, as shown in Figures 5a to 5e. With the larger wall angle θ_{wall} of 20°, the convection cells become reversed (Figure 5f).

Grossman (1997) used the simulation tools to calculate the velocity fields of the granular bed with a different angle of side walls. The current velocity field plots (Figures 2 to 5) agree qualitatively well with Grossman's (1997) simulation results.

When the bed is upward, the particles along the tilted outward side walls have more spaces to expand comparing with the vertical walls (Grossman, 1997). On the contrary, the particles along the tilted outward side walls are in a looser packed condition in comparison to the case using vertical walls. As the tilted angle of the side walls increase to a critical value, the net force exerting on particles changes its direction from

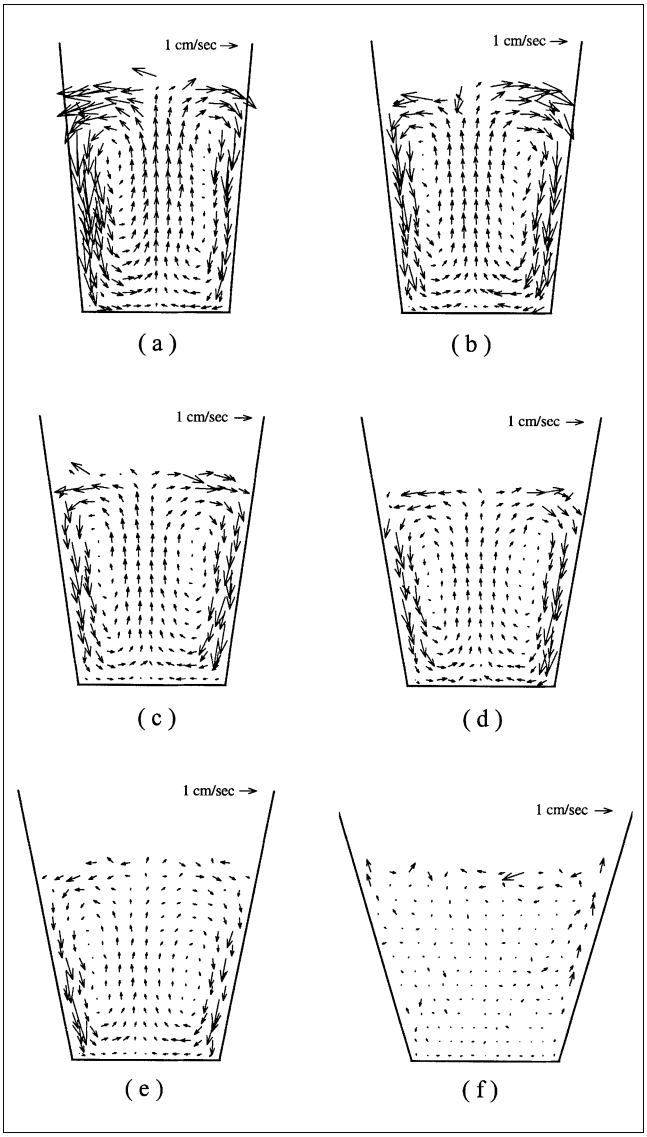

Figure 5. Velocity fields of the granular bed with Wall 3 as side walls rotating outward.

$\Gamma = 4$; $V_b = 2$, θ_{wall} = (a) 6°, (b) 8°, (c) 10°, (d) 12°, (e) 14°, (f) 20°.

downward to upward, which results in the reverse convection cells.

In each convection cell, the disks move around the cell center and the mass-flow rate should be conserved. The horizontal velocity is 0 in the horizontal plane crossing the convection center (Hsiau and Chen, 2000), and only the vertical velocity component V_y exists. Hence, the convection mass-flow rate $\dot{m}$ (per depth) can be defined by

$$\dot{m} = -\mathrm{sgn}\big(V_y(x=W)\big)\int_{x=0}^{x=W}\frac{\rho_p \nu |V_y(x)|}{2}dx \qquad (1)$$

where ν is the solid fraction and W is a half of the container width across the convection center. The sign of the mass-flow rate is determined by the velocity along the side walls. With

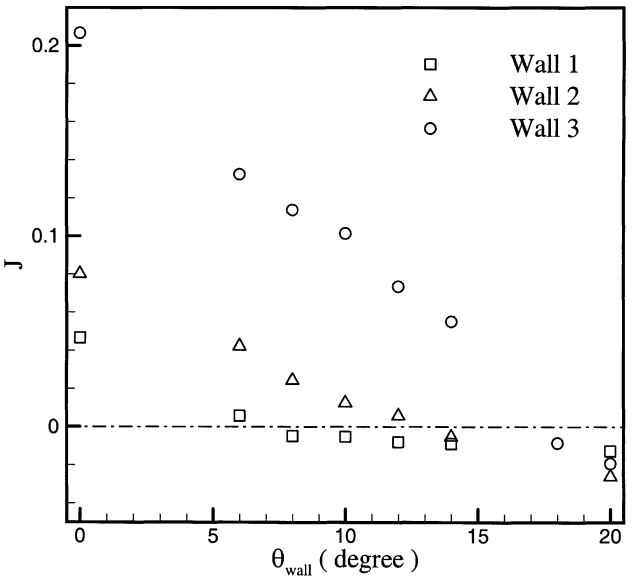

Figure 6. Dimensionless convection flow rate J as a function of the tilted angle of the side walls θ_{wall}.

the downward motion along the side walls, the convection cells are in the normal direction with a positive convection flow rate. For the reverse convection cell, the disks move upward along the side walls with a negative convection flow rate. Assuming that the solid fraction is constant across a horizontal plane, by dividing the channel into experimental bins vertically, the dimensionless convection flow rate J can be expressed by

$$J = \frac{\dot{m}}{\rho_p \nu W\sqrt{gd}} = -\mathrm{sgn}\big[V_y(x=W)\big]\frac{\sum |V_y \Delta x|}{2W\sqrt{gd}} \qquad (2)$$

where Δx is the width of each bin. The dimensionless convection flow rate for the above experimental tests can be calculated from the data in Figures 2 to 5 and Eq. 2. The dimensionless convection flow rate J can be used to characterize the strength of the convection cells. Figure 6 shows the dimensionless convection flow rate J as a function of the tilted angle of the side walls θ_{wall}. The convection flow rates with three different walls decrease with the increase of θ_{wall}, concerning the sign of J. The results are consistent with the experimental results of Knight (1997) and the simulation results of Grossman (1997). There exists a transition angle θ_{tr} for each wall where the convection cells start to reverse. The transition angle of 10° was found by Knight (1997) using 1-mm poppy seeds as granular materials with side walls glued by the same poppy seeds ($\Gamma = 4.2$, $V_b = 2.65$). In the current test, using 4-mm/5-mm mixed disks as granular matter with Wall 2 (glued by 4-mm disks) as side walls, the transition angle is 12° ($\Gamma = 4$, $V_b = 2$). Since the disks in the bed are not in the same size, the friction along the walls would be a little higher than the above case by Knight (1997), which results in the greater transition angle in the current test. Grossman used d_w/d to denote the wall roughness, where d_w is the diameter

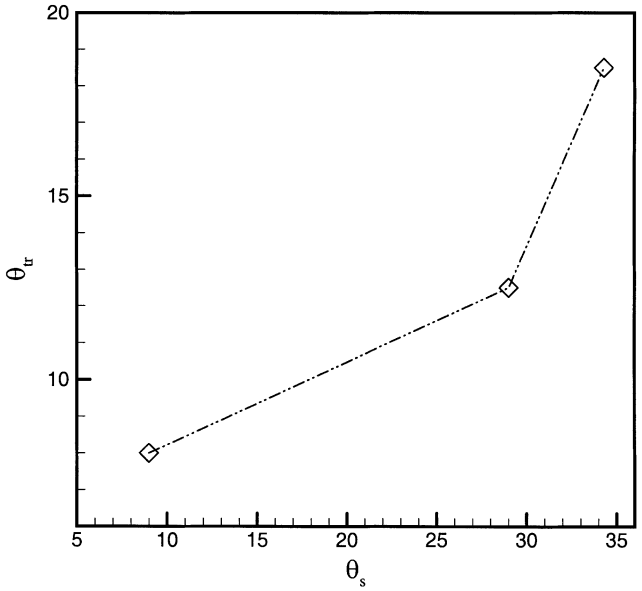

Figure 7. Transition angle θ_{tr} plotting against the sliding angle θ_s of side walls.

of particles glued to the side walls. The transition angle is close to 10° with d_w/d of 1.0 ($\Gamma = 7$, $V_b = 4.65$). In the current test, the d_w/d ranges from 0.8 to 1.2 for Walls 2 and 3 resulting in the transition angles of 12° and 18°, respectively, ($\Gamma = 4$, $V_b = 2$). With the relatively greater Γ and V_b in Grossman's tests, the simulation underpredicts the transition angle, comparing with the experimental tests in this article and in Knight's (1997) article.

Figure 7 shows the transition angle θ_{tr} plotting against the sliding angle θ_s of the side walls. Figure 7 also shows that the convection flow rate is greater for the rougher side walls, since the rougher wall induce the greater shear force resulting in the greater velocities of the granular materials along the side walls. Note, that in order to determine the transition angle of the case using Wall 3, one additional experiment using wall tilted angle $\theta_{\text{wall}} = 18°$ (Wall 3) was performed.

Influences of the vibration velocity

Wall 1 ($\theta_s = 9°$) was chosen as the side walls of the vibrated container in this series of tests. The tilted angles θ_{wall} of 0° and 20° were tested. The dimensionless acceleration was fixed at 4 and the dimensionless velocity amplitudes V_b of 1.32, 1.48, 1.69, 2.00, and 2.28 were used.

Figures 8a to 8e show the velocity fields of the disks in the rectangular container ($\theta_{\text{wall}} = 0°$) with the five different vibration velocities. The normal convection cells exist in all cases and the convection strength increases with the vibration velocity amplitude. The velocity fields of granular disks in the container with θ_{wall} of 20° are shown in Figures 9a to 9e. Similarly, the convection strength increases with the vibration velocity amplitude, but the directions of the convection cells are reversed.

The dimensionless convection flow rate J can be calculated using Eq. 2. The relation of J and V_b using the two different containers ($\theta_{\text{wall}} = 0°$ and 20°) are shown in Figure 10. The convection strength (absolute values of J) increase

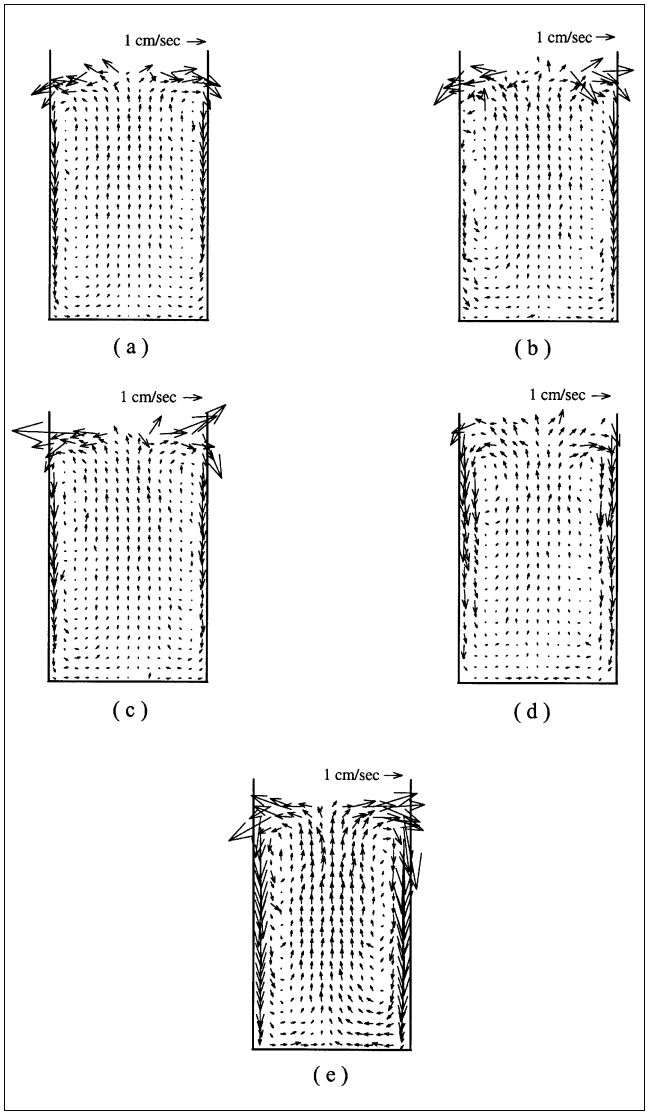

Figure 8. Velocity fields of the disks in the rectangular container ($\theta_{\text{wall}} = 0°$).

Dimensionless velocity amplitude V_b of (a) 1.32, (b) 1.48, (c) 1.69, (d) 2.00 and (e) 2.28 (Wall 1, $\Gamma = 4$).

with the increase of V_b. A similar conclusion is shown in Figure 12 of Grossman's (1997) article. Note that the parameter used by Grossman's article is the frequency f under the same Γ, and $f \propto 1/V_b$.

Influences of the convection on disk segregation

As stated in the Introduction, there are two possible mechanisms causing the segregation of granular materials in a shaker: particle reorganization and convection cells. Since there are different container geometry results in the different direction of convection cells, it is interesting to investigate the disk segregation phenomena in these different containers.

The experimental setup was similar to the first set of experiments, but there was a larger disk (30 mm in diameter, same material and thickness as the smaller disks) placed in the middle of the container before the experiment. The di-

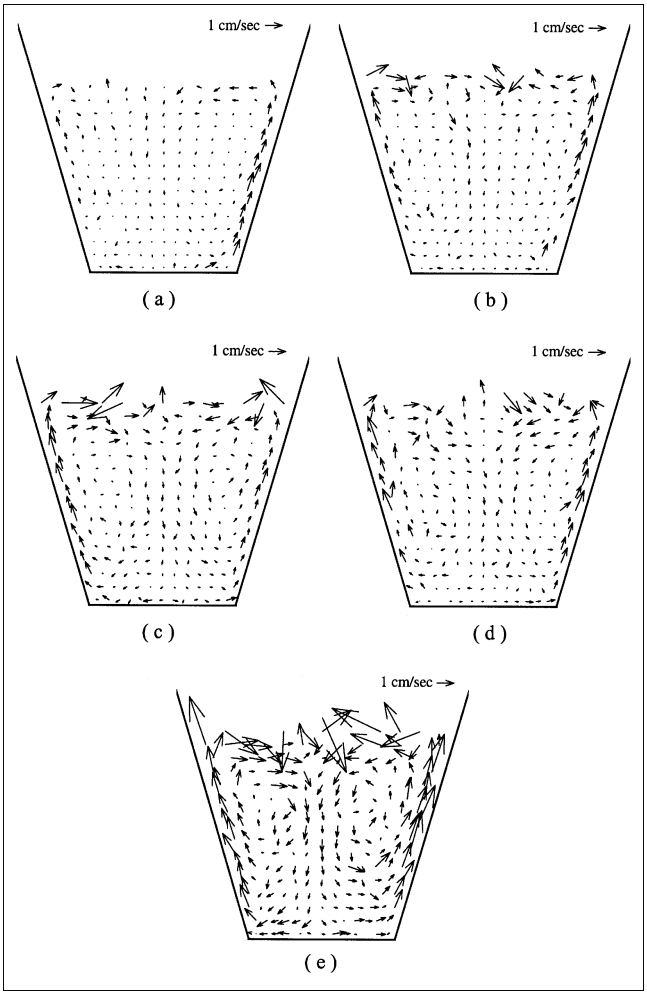

Figure 9. Velocity fields of the disks in the container of $\theta_{wall} = 20°$.

Dimensionless velocity amplitude V_b of (a) 1.32, (b) 1.48, (c) 1.69, (d) 2.00 and (e) 2.28 (Wall 1, $\Gamma = 4$).

mensionless vibration acceleration and velocity were also fixed at $\Gamma = 4$ and $V_b = 2$. Seven containers with different tilted angles of side walls, θ_{wall} (0°, 6°, 8°, 10°, 12°, 14°, and 20°) and different materials of side walls (sliding angles θ_s of 9°, 29°, and 34.3°) were tested. One more container of a tilted angle of 18° was used for the case of Wall 3.

Figure 11 shows the heights of the large disk in the container vs. time, using Wall 2 ($\theta_s = 29°$) as side walls. The larger disk can rise up to the top with θ_{wall} of 0°, 6°, 8°, and 10°. The time for the larger disk reaching to the top increases with θ_{wall}. Using the container with θ_{wall} of 12°, the larger disk cannot move to the top in a relatively long time. The larger disk even moves downwards when θ_{wall} of 14° and 20° are used. The larger disk can get to the bottom in 25 s with θ_{wall} of 20°.

The vertical velocity of the larger disk during its rising or sinking process V_{large} can be calculated from Figure 11 by a first-order curve fitting using a least-squares method. Figure 12 shows the vertical velocity of the larger disk V_{large}, plotting against the angle of the side walls θ_{wall} by using Walls 1, 2, and 3 as side walls. The rising velocity decreases with the wall angle and becomes negative when the side angle is greater than a transition value.

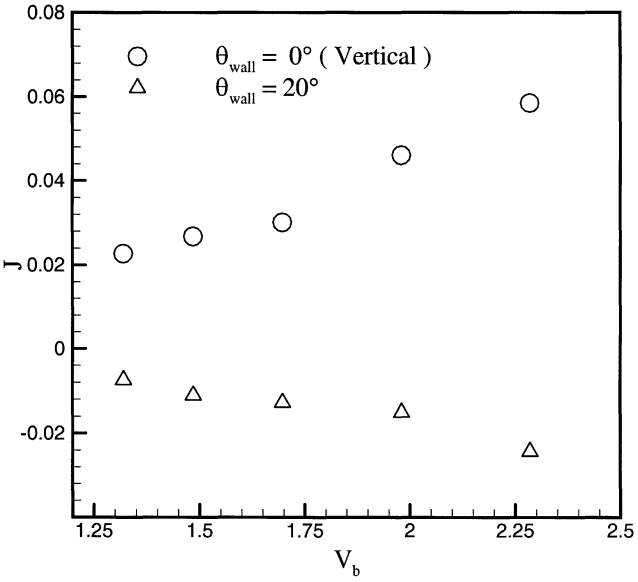

Figure 10. Dimensionless convection flow rate J as a function of the dimensionless velocity amplitude V_b.

Figure 13 shows the vertical velocity of the larger disk V_{large} plotting against the dimensionless convection flow rate J by using Walls 1, 2 and 3 as side walls. The preliminary tests showed that the convection flow rate J was very insensitive to the presence of the single larger disk. Thus, we analyzed the effect of the convection flow rate J on the segregation using the data of J from the above experiments with no larger disk presented in the bed. The rising velocity of the larger

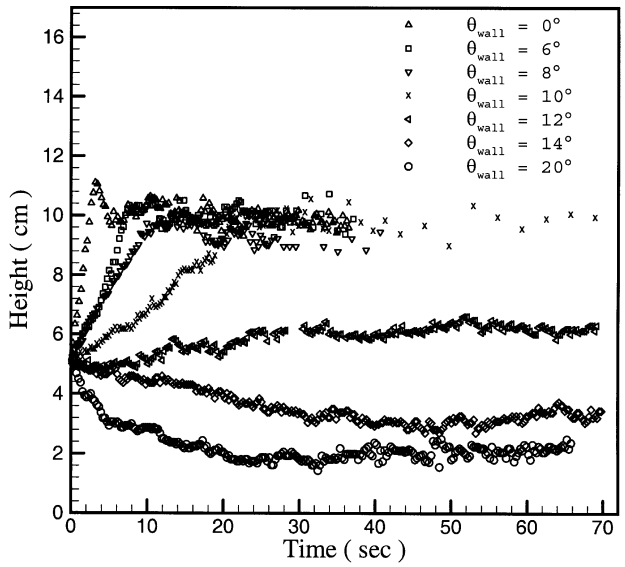

Figure 11. Heights of the large disk in the container versus time, using Wall 2 as side walls.

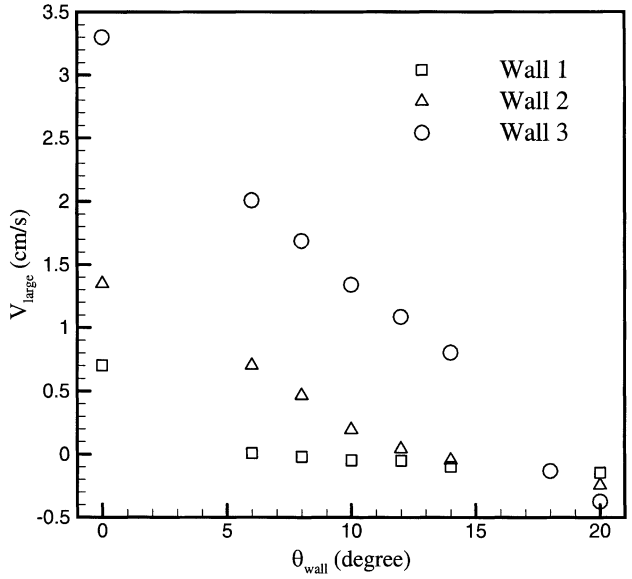

Figure 12. Vertical velocity of the large disk V_{large}, plotting against the angle of side wall θ_{wall}, by using Walls 1, 2, and 3.

disk increases with the dimensionless convection flow rate. The upward motions of the smaller disks in the central bed (the normal convection cells, positive J) can bring the larger disk to the top. On the contrary, the larger disk can follow the smaller disks in the central bed to the bottom when the reverse convection cells exist in the bed (negative J). Also, the 0 convection flow rate cannot make the larger disk move upward nor downward, resulting in the 0 value of V_{large}. The rising velocities V_{large} for the three different wall roughness correlate very well with the dimensionless convection flow rates J and their relation is linear. It indicates that the segregation process is strongly dependent on the convection cells in the bed.

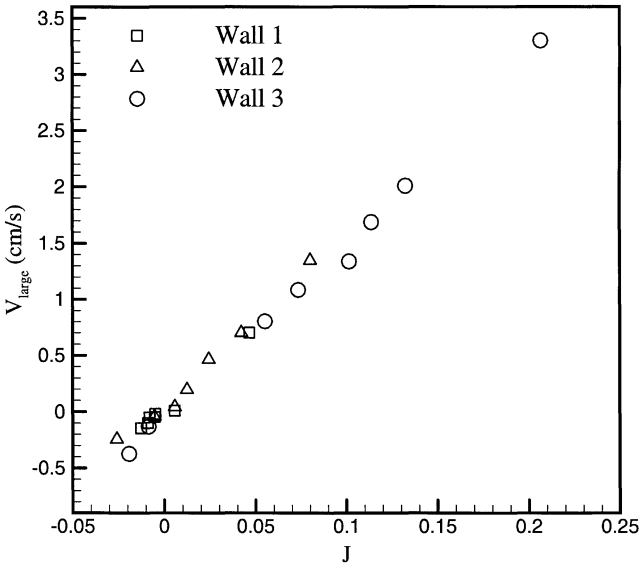

Figure 13. Vertical velocity of the large disk V_{large}, plotting against the dimensionless convection flow rate J by using Walls 1, 2, and 3.

As stated before, "particle reorganization" and "bed convection" are two important mechanisms causing the segregation of particles in a vibrated bed. There are many debates about the importance and the domination between these two mechanisms. From the current study, with the same vibrated conditions under different container geometry, the larger disk may rise up to the top or sink to the bottom. The mechanism of disk reorganization seems to fail to explain the sinking of the large disk. Figure 13 does show the monotonous and linear dependence of the separation velocity on the convection flow rate. It seems that we can draw the conclusion that the convection cell of the smaller disks is the dominant cell, and probably the only mechanism causing the separation of the larger disk.

However, it may not be right to drive to the conclusion that the particle reorganization is nothing to do with the particle separation in a vibrated bed. The current experiment is a 2-D experiment where a 2-D shaker and 2-D disks are used. For the disks, the solid fraction of granules is relatively high and it is not easy to reach the expansion state of the bed resulting in the difficulty of disk reorganizations. Thus, the convection cell of the smaller disk becomes the dominant mechanism in the segregation process. However, for a 3-D bed with spherical particles, the role of particle reorganization may be important. The studies for a 3-D granular bed are currently undergoing in our laboratory in order to have the advanced conclusions in the future.

Conclusion

The effect of container geometry on the convection cell phenomena in a vibrated granular bed was investigated experimentally. Two convection cells existed symmetrically in the bed. The directions of the convection cells were reversed when the angle of the side walls was greater than a transition value. The convection flow rate decreases with the increase of the tilted angle of the side walls. With the same vibration acceleration, the greater vibration velocity resulted in the higher convection strength (absolute value). In the current 2-D experiment the convection cells of the smaller disks played the dominant role in the segregation process of the larger disk. The direction and the strength of the convection cells determined the movement of the larger disk in the bed. The segregation velocity was monotonously dependent on the convection flow rate in a linear relation.

Acknowledgment

The authors would like to acknowledge the support from the National Science Council of the R.O.C. for this work through grant NSC-89-2211-E-008-018.

Literature Cited

Barker, G. C., and A. Metha, "Size Segregation Mechanisms," *Nature*, **364**, 486 (1993).

Clément, E., J. Duran, and J. Rajchenbach, "Experimental Study of Heaping in a Two-Dimensional Sandpile," *Phys. Rev. Lett.*, **69**, 1189 (1992).

Clément, E., and J. Rajchenbach, "Fluidization of a Bidimensional Powder," *Europhys. Lett.*, **16**, 138 (1991).
Douady, S., S. Fauve, and C. Laroche, "Subharmonic Instabilities and Defect in a Granular Layer under Vertical Vibrations," *Europhys. Lett.*, **8**, 621 (1989).
Evesque, P., and J. Rajchenbach, "Instability in a Sand Heap," *Phys. Rev. Lett.*, **69**, 44 (1989).
Fauve, S., S. Douady, and C. Laroche, "Collective Behaviors of Granular Masses under Vertical Vibration," *J. Phys. (Paris)*, **50**, 187 (1989).
Gallas, J. A. C., H. J. Herrmann, and S. Sokolowski, "Convection Cells in Vibrating Granular Media," *Phys. Rev. Lett.*, **69**, 1371 (1992).
Grossman, E. L., "Effects of Container Geometry on Granular Convection," *Phys. Rev. E*, **56**, 3290 (1997).
Hayakawa, H., S. Yue, and D. C. Hong, "Hydrodynamic Description of Granular Convection," *Phy. Rev. Lett.*, **75**, 2328 (1995).
Hsiau, S. S., and C. H. Chen, "Granular Convection in a Vertical Shaker," *Powder Technol.*, **111**, 210 (2000).
Hsiau, S. S., and S. J. Pan, "Motion State Transitions in a Vibrated Granular Bed," *Powder Technol.*, **96**, 219 (1998).
Hsiau, S. S., and Y. M. Shieh, "Fluctuations and Self-Diffusion of Sheared Granular Material Flows," *J. Rheol.*, **43**, 1049 (1999).
Hsiau, S. S., M. H. Wu, and C. H. Chen, "Arching Phenomena in a Vibrated Granular Bed," *Powder Technol.*, **99**, 185 (1998).
Hsiau, S. S., and H. Y. Yu, "Segregation Phenomena in a Shaker," *Powder Technol.*, **93**, 83 (1997).
Ichiki, K., and H. Hayakawa, "Dynamical Simulation of Fluidized Beds Hydrodynamically Interacting Granular Particles," *Phys. Rev. E*, **52**, 658 (1995).
Jaeger, H. M., and S. R. Nagel, "Physics of the Granular State," *Science*, **255**, 1523 (1992).
Jullien, R., P. Meakin, and A. Pavlovitch, "Three-Dimensional Model for Particle-Size Segregation by Shaking," *Phys. Rev. Lett.*, **69**, 640 (1992).
Knight, J. B., "External Boundaries and Internal Shear Bands in Granular Convection," *Phys. Rev. E*, **55**, 6016 (1997).
Knight, J. B., E. E. Ehrichs, V. Y. Kuperman, J. K. Flint, H. M. Jaeger, and S. R. Nagel, "Experimental Study of Granular Convection," *Phys. Rev. E*, **54**, 5726 (1996).
Knight, J. B., H. M. Jaeger, and S. R. Nagel, "Vibration-Induced Size Separation in Granular Media: the Convection Connection," *Phys. Rev. Lett.*, **70**, 3728 (1993).
Knight, J. B., H. M. Jaeger, and S. R. Nagel, "Granular Convection and Size Separation," *Book of Abstracts McNU'97, the 1997 Joint ASME, ASCE, SES Summer Meeting*, Northwestern University, p. 616 (1997).
Laroche, C., S. Douady, and S. Fauve, "Convective Flow of Granular Masses under Vertical Vibrations," *J. Phys. (Paris)*, **50**, 699 (1990).
Lee, J., "Heap Formation in Two-Dimensional Granular Media," *J. Phys. A*, **27**, L257 (1994).
Luding, S., E. Clément, A. Blumen, J. Rajchenbach, and J. Duran, "Onset of Convection in Molecular Dynamics Simulations of Grains," *Phys. Rev. E*, **50**, 1762 (1994).
Melo, F., P. Umbanhowar, and H. Swinney, "Transition to Parametric Wave Patterns in a Vertically Oscillated Granular Layer," *Phys. Rev. Lett.*, **72**, 172 (1994).
Natarajan, V. V. R., M. L. Hunt, and E. D. Taylor, "Local Measurements of Velocity Fluctuations and Diffusion Coefficients for a Granular Material Flow," *J. Fluid Mech.*, **304**, 1 (1995).
Pak, H., and R. Behringer, "Surface Waves in Vertically Vibrated Granular Materials," *Phys. Rev. Lett.*, **71**, 1832 (1993).
Pakowski, Z., A. S. Mujumdar, and C. Strumillo, "Theory and Application of Vibrated Beds and Vibrated Fluid Beds for Drying Processes," *Advances in Drying 3*, A. S. Mujumdar, ed., Hemisphere, Washington, DC, pp. 85–99 (1984).
Rosato, A., K. J. Strandburg, and R. H. Swendsen, "Why the Brazil Nuts are on Top: Size Segregation of Particulate Matter by Shaking," *Phys. Rev. Lett.*, **58**, 1038 (1987).
Suzuki, K., H. Hosaka, R. Yamazaki, and G. Jimbo, "Drying Characteristics of Particles in a Constant Drying Rate Period in Vibro-Fluidized Bed," *J. Chem. Eng. Japan*, **13**, 117 (1980).
Taguchi, Y. H., "New Origin of Convective Motion: Elastically Induced Convection in Granular Materials," *Phys. Rev. Lett.*, **69**, 1367 (1992).
Warr, S., J. M. Huntley, and G. T. H. Jacques, "Fluidization of a 2-Dimensional Granular System—Experimental Study and Scaling Behavior," *Phys. Rev. E*, **52**, 5583 (1995).
Wassgren, C. R., M. L. Hunt, and C. E. Brennen, "Vertical Side Wall Convection in Deep Beds of Granular Materials Subjected to Vertical Vibration," *Proc. of 5th World Congress of Chem. Eng.*, San Diego, CA, 355 (1996).
Wassgren, C. R., "Vibration of Granular Materials," PhD Thesis, California Institute of Technology, CA (1997).
Yu, S. H., B. J. Ma, and Y. Q. Weng, "Drying Performance and Heat Transfer in a Vibrated Fluidized Beds," *Drying '92*, A. S. Mujumdar, ed., Elsevier, Amsterdam, pp. 731–740 (1992).

Manuscript received June 8, 2000, and revision received Dec. 7, 2001.